J Low Temp Phys (2017) 187:618–626
DOI 10.1007/s10909-016-1713-7

Exploding and Imaging of Electron Bubbles in Liquid Helium

Neha Yadav[1] · Vaisakh Vadakkumbatt[1] · Humphrey J. Maris[2] · Ambarish Ghosh[1,3]

Received: 27 July 2016 / Accepted: 16 November 2016 / Published online: 28 November 2016

Abstract An electron bubble in liquid helium-4 under the saturated vapor pressure becomes unstable and explodes if the pressure becomes more negative than −1.9 bars. In this paper, we use focused ultrasound to explode electron bubbles. We then image at 30,000 frames per second the growth and subsequent collapse of the bubbles. We find that bubbles can grow to as large as 1 mm in diameter within 2 ms after the cavitation event. We examine the relation between the maximum size of the bubble and the lifetime and find good agreement with the experimental results.

Keywords Cavitation 1 · Single electron bubbles 2 · Superfluid helium 3

1 Introduction

The two electrons in a neutral helium atom occupy a filled shell. As a result, an electron is strongly repelled from a helium atom due to the Pauli exclusion principle. If an extra electron is injected into liquid helium, a hollow cavity is formed and the electron is localized inside this cavity. This structure is referred to as a single electron bubble. These electron bubbles form a powerful system for studying the quantum properties of an electron and have been investigated theoretically and experimentally for many years [1]. The lowest energy configuration of the bubble is with the electron in the 1S ground state with a wave function which, to a good approximation, is close to zero

✉ Neha Yadav
nehayadav@physics.iisc.ernet.in

1 Department of Physics, Indian Institute of Science, Bangalore 560012, India

2 Physics Department, Brown University, Providence, RI, USA

3 Centre for Nano Science and Engineering, Indian Institute of Science, Bangalore 560012, India

at the bubble wall. The electron can be excited to other states, such as 1P and 2P, using light of the appropriate wavelength [2–5]. The bubbles can become trapped on quantized vortices [6], and if the bubble velocity is made sufficiently large as a result of the application of an electric field, the moving bubbles create vortices and become trapped on them [7].

The energy of a single electron bubble in the ground state can be written as the sum of the quantum zero-point energy, the surface energy, and the work done against the pressure P in the liquid. Thus,

$$E = \frac{h^2}{8mR^2} + 4\pi R^2\alpha + \frac{4}{3}\pi R^3 P, \tag{1}$$

where m is the mass of an electron and α is the surface tension of the liquid helium at the given temperature. The correction due to the potential barrier penetration and polarizability [10] is very small and hence being ignored in the equation shown above.

For zero applied pressure, the equilibrium radius $R_{\min}$ at which the energy of the bubble is a minimum is given by

$$R_{\min} = \left(\frac{h^2}{32\pi m\alpha}\right)^{1/4} \tag{2}$$

At zero temperature, this is 1.9 nm. When the temperature is increased, $R_{\min}$ decreases due to the decrease in the surface tension. If a positive pressure is applied to the bubble, the size of the bubble decreases. If the applied pressure is negative, $R_{\min}$ increases and beyond a critical pressure P_c, given by [8]

$$P_c = -\frac{16}{5}\left(\frac{2\pi m}{5h^2}\right)^{1/4}\alpha^{5/4}, \tag{3}$$

there is no longer a radius at which the bubble is stable [9]. At zero temperature P_c is -1.9 bars, and at higher temperatures the magnitude of P_c decreases because of the temperature variation of surface tension. For any pressure that is negative with respect to P_c, the bubble starts to grow rapidly, and so P_c is known as the cavitation pressure.

In previous experiments, measurements have been made of the critical pressure and how it varies with temperature [10]. A focused sound wave was used to produce an oscillating pressure, and the onset of cavitation was found by detecting the light scattered from the cavitation bubbles. The change in the critical pressure that occurs when the bubble becomes attached to a vortex [10] and when the electron is excited to higher quantum state has also been measured [11].

Roche et al. [12] have developed a method to estimate the size of bubbles (bubbles not containing an electron) as a function of the time after the explosion. In their experiment, a beam of light was passed through the region near to the acoustic focus. Light that was incident on a bubble was scattered through an angle large enough to prevent it reaching the photomultiplier used for detection. Thus, from the reduction in the PMT signal the time dependence of the size of the bubbles could be determined. Bubbles of maximum radius as large as 90 μm were detected in this way. In the present

work, we use a high-speed camera to directly image the cavitation bubbles and measure their shape and size as a function of time.

2 Experimental Setup and Result

The experimental setup is shown in Fig. 1. Sound pulses of frequency 1 MHz were generated using a PZT-4 transducer driven for 10 μs. The transducer (outer diameter of 11.6 mm) was slightly less than a hemisphere making it possible to view the acoustic focus directly. For injecting the electrons inside the liquid helium, a Ni-63 radioactive source was used. The level of helium in the cell was slightly above the grid, touching the radioactive source. The radioactive source was housed inside a brass mount, and by applying a voltage, the density of electrons near the acoustic focus could be adjusted. To further control the electron density, a mesh with 2800 wires per meter on a brass ring was employed. The radioactive source and mesh were normally kept at potentials of −500 V and −200 V, respectively. When the two were kept at a positive voltage, no events were observed. The distance between the radioactive source and transducer focus was 0.005 m. For imaging the event, a Photron high-speed camera (model SA4) was operated at a frame rate of 30,000 frames per second. Illumination was achieved by means of an LED array, together with an additional lens which is not shown in the figure. The experiments were carried out within the temperature range 1.5–2.5 K.

In the videos, the growth and collapse of the bubble could be easily observed. Figure 2 shows frames from one of the videos that were recorded at 1.8 K with a voltage of 140 V applied to the transducer. A MATLAB code was used to fit an ellipse to the bubble shape as recorded in each frame, and the lengths of the major and minor axes and their orientation were calculated. As is evident from Fig. 2, initially the major axis lies close to the vertical direction. The bubble grows with time and at one point is almost spherical in shape. During the collapse, the major axis ends up in the horizontal direction. After the collapse of the bubble, sometimes a second bubble is produced (not shown in this video). Figure 3a shows the lengths of the major and minor axes of the

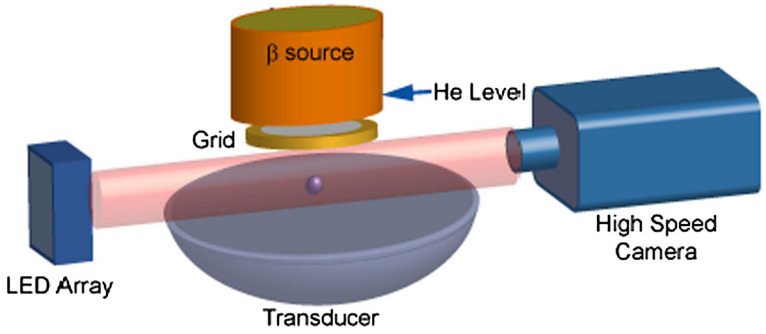

Fig. 1 Schematic diagram of the apparatus. The radioactive source was used to inject electrons inside liquid helium. A grid with a mesh of 2800 wires per meter was used to control the electron density. A sine wave of 1 MHz was applied to the transducer for 10 μs for producing the sound pulse (Color figure online)

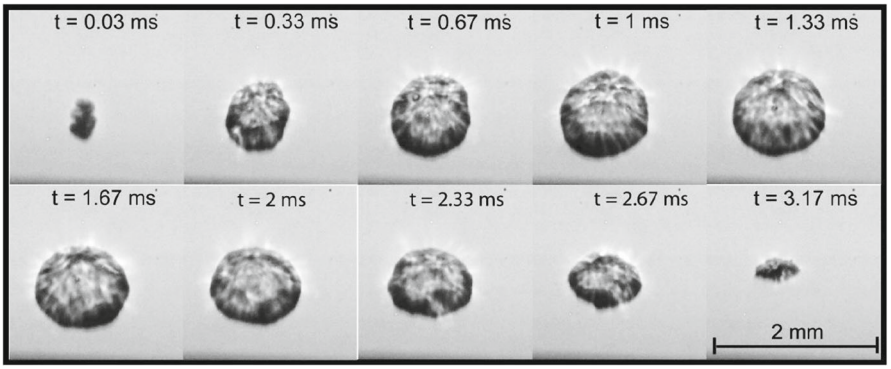

Fig. 2 Series of images of a bubble exploded at 1.8 K. The video was taken using LED illumination and a high-speed camera running at 30,000 fps

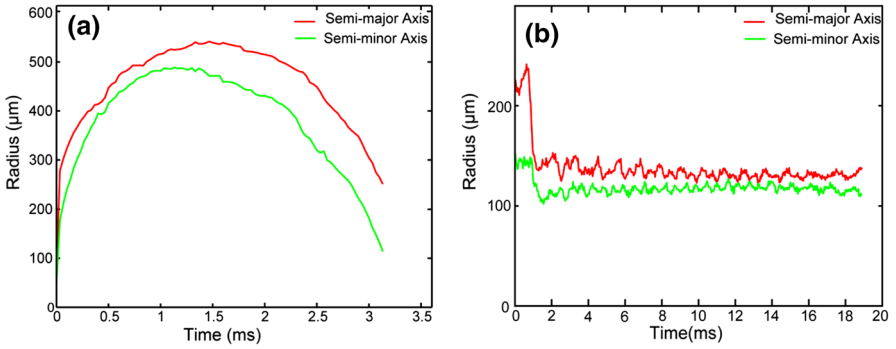

Fig. 3 **a** Semimajor and semiminor axes as a function of time for the bubble shown in Fig. 2. Note that nucleation occurs about 0.1 ms before the zero of time indicated on the axis. **b** Semimajor axis for the bubble exploded shown in Fig. 4. Note that nucleation occurs about 0.1 ms before the zero of time indicated on the axis (Color figure online)

ellipse as a function of time. The maximum values of the semimajor and semiminor axes are 540 and 480 μm, respectively.

The same experiment was performed at temperatures above the lambda point. The video in Fig. 4 was taken at 2.4 K, again with a voltage of 140 V applied to the transducer. The bubble first tumbles and rotates, but as time proceeds it becomes more stable. It starts to rise up because of buoyancy and eventually escapes the field of view. Figure 3b shows the variation of bubble size and shape with time. The bubble quickly reaches its maximum size and then rapidly shrinks to roughly half of its maximum size. After this point, the major axis decreases very slowly while the bubble becomes closer to being round. Its lifetime is much longer than the lifetime at 1.8 K. The analysis indicates that there are small-amplitude periodic oscillations in the major and minor axis. These are of unknown origin and are only marginally above the noise. The final collapse of the bubble is not observed because the bubble escapes the field of view before this happens.

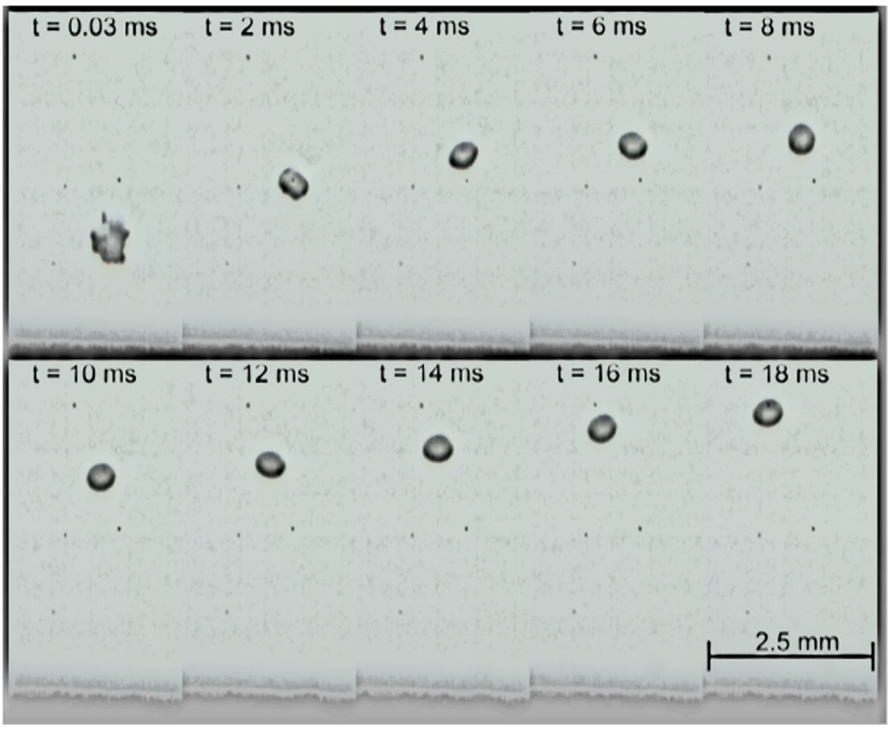

Fig. 4 Series of images of a bubble exploded at 2.4 K. The video was taken using a high-speed camera and LED array at 30,000 fps (Color figure online)

Some general features of these results are easy to understand. Although the pressure field of the sound has axial symmetry, the electron bubble that explodes is unlikely to lie exactly on the axis; this explains why the bubble shape at later times does not have axial symmetry. Immediately after the bubble explodes, the bubble size will be small compared to the distance over which the pressure varies; this distance is of the order of 40 μm (the sound wavelength divided by 2π). Up to this point, the shape should remain spherical, but at this stage of the expansion the bubble is too small for us to record an image. Once the bubble exceeds this size, there will be different pressures exerted on different parts of the bubble surface. In addition, the presence of the bubble will substantially modify the sound field.

Given these issues, it is hard to make a detailed analysis of the bubble shape and evolution. However, as we will now discuss it is very interesting to consider how it is possible for the sound field to lead to bubbles as large as we have detected. Consider first the results obtained in superfluid helium. The rate at which work is done on the bubble by the pressure field P_{sound} must balance the rate of change of energy of the bubble, i.e., the sum of the kinetic energy of the liquid flowing away, the surface energy and the zero-point energy of the electron. Thus,

$$-4\pi R^2 \dot{R} P_{\text{sound}} = \frac{d}{\text{dt}} \left(2\pi \rho R^3 \dot{R}^2 + 4\pi R^2 \alpha + \frac{h^2}{8mR^2} \right). \tag{4}$$

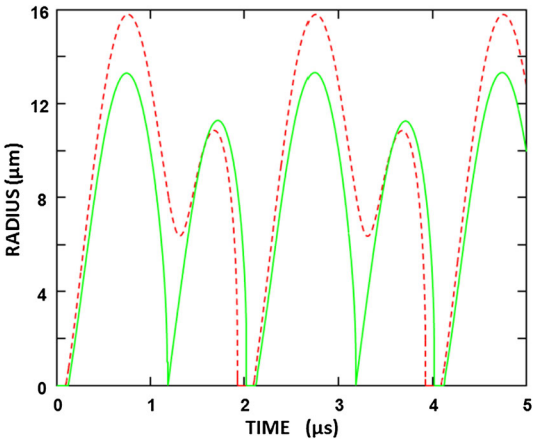

Fig. 5 Results of a calculation of the radius as a function of time for a sound field as described in the text. The *solid curve* is for an oscillation amplitude of 2 bars, and the *dashed curve* is for an amplitude of 2.5 bars (Color figure online)

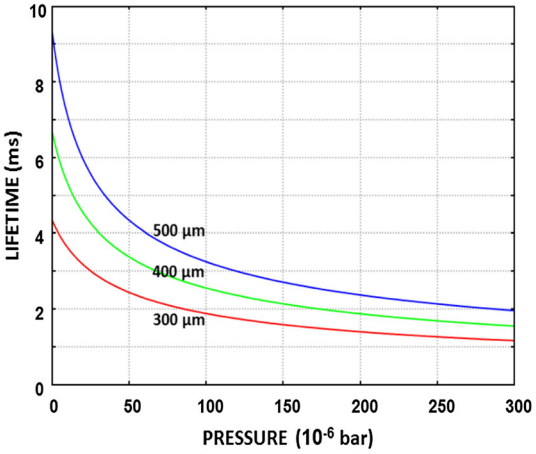

Fig. 6 Calculated lifetime of bubbles of maximum radius 300, 400, and 500 μm as a function of the applied pressure (P_0) (Color figure online)

This neglects any effects due to the compressibility and viscosity of the liquid. The effect of compressibility depends on the timescale/bubble size that is being considered. It is certainly important for nanometer-size bubbles. But for the data in Fig. 3a, the maximum velocity of the bubble wall is of the order of 0.5 m/s which is small compared to the sound velocity. Thus, the possible effect of compressibility is limited to the initial growth stage. This leads to the following generalization of the Rayleigh–Plesset [13] equation that allows for the presence of the electron:

$$\ddot{R} = -\frac{3\dot{R}^2}{2R} - \frac{2\alpha}{\rho R^2} + \frac{h^2}{16\pi m \rho R^6} - \frac{P_{\text{sound}}}{\rho R}. \tag{5}$$

In Fig. 5, we show the results of simulations of the bubble size under the influence of sinusoidal 1 MHz pressure oscillations with amplitude 2 and 2.5 bars; this is the approximate pressure range used in the present experiments. The density is 145 kg m^{-3}, and the surface tension is 3.16×10^{-4} Nm^{-1}. For simplicity, it has been assumed in

the simulation that when the bubble collapses we can ignore the "bounce," i.e., the formation of a new bubble immediately after the collapse. We do this in the first place because Eq. 5 does not hold when the radius becomes very small, e.g., a few Å, since then the energy of the electron becomes larger than the potential barrier normally faced by an electron entering the liquid. In the second place, it is known that when a bounce does occur a significant part of the energy is lost, whereas Eq. 5 is based upon energy conservation. But, nevertheless, in the discussion below, we reconsider the possibility that a bounce is important.

From the simulation, we see that for the pressures considered the largest radius reached is only 16 μm. The bubble grows rapidly to this size but then collapses when the applied pressure returns to a positive value. The maximum radius is much smaller than the maximum radius found in the experiment. We therefore investigate the possibility that at some point while the bubble is growing rapidly under the action of the negative pressure swing, the bubble moves out of the transducer focus very fast, perhaps as a result of radiation pressure, to a location where the pressure oscillation is much smaller. The bubble would then continue to expand because of the kinetic energy of the outflowing liquid around it.

The first question then is whether this energy is sufficient to produce the bubbles we see. Suppose that the maximum kinetic energy occurs when the radius is R_0 and the velocity is $\dot{R}_0$. Let the pressure in the liquid at the new location of the bubble be P_0. Then the maximum radius $R_{\max}$ the bubble can reach is given by

$$K = 2\pi\rho R_0^3 \dot{R}_0^2 = 4\pi R_{\max}^2 \alpha + \frac{4\pi}{3} R_{\max}^3 P_0. \tag{6}$$

So if, for example, $P_0 = 0$ then in order to have $R_{\max} = 500\,\mu\text{m}$ we need to have $R_0^3\dot{R}_0^2$ at least 1.1×10^{-12} m^5 s^{-2}. From the results in Fig. 5, we find that the maximum values of $R_0^3\dot{R}_0^2$ are 1.2×10^{-12} and 7×10^{-13} m^5 s^{-2} for maximum pressures of 2.5 and 2 bars, respectively. Thus, the energy is in the right general range to explain the bubbles we see but it may be that the extra energy resulting from the bounce may need to be considered.

As a test, we can consider the relation between $R_{\max}$ and the lifetime of the bubble. Using Eq. 5, it is straightforward to show that when the bubble has radius R the surface velocity is

$$\dot{R} = \sqrt{\frac{2\alpha}{\rho}\left(\frac{R_{\max}^2}{R^3} - \frac{1}{R}\right) + \frac{2P_0}{3\rho}\left(\frac{R_{\max}^3}{R^3} - 1\right)}. \tag{7}$$

Then the lifetime is

$$T = 2\int_0^{R_{\max}} \frac{\mathrm{d}R}{\sqrt{\frac{2\alpha}{\rho}\left(\frac{R_{\max}^2}{R^3} - \frac{1}{R}\right) + \frac{2P_0}{3\rho}\left(\frac{R_{\max}^3}{R^3} - 1\right)}}. \tag{8}$$

If the pressure is zero, then

$$T = 1.236\frac{\rho^{1/2} R_{\max}^{3/2}}{\alpha^{1/2}}, \tag{9}$$

whereas if the surface tension is neglected

$$T = 1.829 \frac{\rho^{1/2} R_{\max}}{P_0^{1/2}} \tag{10}$$

In Fig. 6, we show the calculated lifetime as a function of P_0 and allowing for surface tension for bubbles of maximum size 300, 400 and 500 μm. This can be compared with the experimental data shown in Fig. 3, where the bubble of maximum size around 500 μm can be seen to collapse around 3.5 ms. For the theory and experimental data to be consistent, the static pressure in the liquid needs to be around 8×10^{-5} bar, which corresponds to the liquid surface to be about 6 mm above the acoustic focus. Due to limited visibility of the experimental setup, we could not measure the exact height of the liquid surface, although we are sure that the height was greater than 4 mm. The comparison between the experiment and theory is further complicated due to non-sphericity of the bubbles imaged in the experiment, while the theoretical calculation assumes the bubbles to be spherical. We hope to measure the lifetime of the bubbles as a function of liquid height in future.

Finally, we mention the behavior of the bubbles above the lambda point. We have not carried out a detailed analysis but need to mention an interesting possibility. During the expansion phase of the bubble, helium atoms evaporate from the bubble wall; they later condense as the bubble collapses. During the evaporation phase, latent heat has to be extracted from the liquid, thereby cooling the liquid near the surface; as the bubble collapses, heat has to be conducted away from the surface into the liquid. In a classical liquid, the times for both growth and collapse of the bubble are affected by the thermal conductivity of the liquid. Since liquid helium above the T_λ is a poor conductor of heat, the collapse time can be much larger than the time that would result just from the inertia of the liquid. However, for a superfluid, the thermal conductivity is essentially infinite and so heat conduction does not limit the growth or collapse rate, i.e., at all times the bubble will contain vapor at close to the saturated vapor pressure. In fact, this has been implicitly assumed in the calculations already presented. Above the lambda point, it seems possible that after the bubble is nucleated the evaporation from the wall may result in a layer of liquid at the bubble surface to be cooled below T_λ. This layer will then be highly conducting and provide a heat source enabling evaporation to continue. However, during the collapse this superfluid layer may disappear and the rate of condensation of the vapor will be very slow because of the low thermal conductivity of normal liquid helium.

3 Summary

Using a high-speed camera system, we have been able to record images showing the growth and collapse of cavitation bubbles in normal and superfluid helium-4. We have proposed a mechanism to explain the large size of the bubbles that are produced. We find that above the lambda point the time taken for bubbles to collapse is much larger than the time for below T_λ, and discuss a possible explanation for this.

Acknowledgements This work was supported by Nanomission, Science and Engineering Research Board, India, by the US National Science Foundation through Grant No. GR5260053, and by the Julian Schwinger Foundation Grant JSF-15-05-0000. The usage of the facilities in Micro and Nano Characterization Facility (MNCF, CeNSE) at IISc is gratefully acknowledged, and the work is partially supported by the Ministry of Communication and Information Technology under a grant for the Centre of Excellence in Nanoelectronics, Phase II.

References

1. H.J. Maris, J. Phys. Soc. Japan **77**, 111008 (2008)
2. C.C. Grimes, G. Adams, Phys. Rev. B **41**, 6366 (1990)
3. C.C. Grimes, G. Adams, Phys. Rev. **B 45**, 2305 (1992)
4. A.Y. Parshin, S.V. Pereverzev, J. Exp. Theor. Phys. Lett. **52**, 282 (1990)
5. C.L. Zipfel, T.M. Sanders, in *Proceedings of the 11th International Conference on Low Temperature Physics*, ed. by J.F. Allen, D.M. Finlayson, D.M. McCall (St. Andrews University, St. Andrews, 1969), p. 296
6. G.W. Rayfield, F. Reif, Phys. Rev. **136**, A1194 (1964)
7. R.J. Donnelly, *Quantized Vortices in Helium II* (Cambridge, London, 1991)
8. V.A. Akulichev, Y.Y. Boguslavskii, Sov. Phys. JETP **35**, 1012 (1972)
9. J. Classen, C.K. Su, H.J. Maris, Phys. Rev. Lett. **77**, 2006 (1996)
10. J. Classen, C.K. Su, M. Mohazzab, H.J. Maris, Phys. Rev. B **57**, 3000 (1998)
11. D. Konstantinov, H.J. Maris, Phys. Rev. Lett. **90**, 025302 (2003)
12. P. Roche et al., Czech. J. Phys. **46**, 381 (1996)
13. W. Lauterborn, T. Kurz, Rep. Prog. Phys. **73**, 106501 (2010)